03,05,07

Kinetic characteristics of the heterogeneous alloy $Cd_3As_2(MnAs)_{0.03}$ at high pressure

© L.A. Saypulaeva [1], A.I. Ril [2], S.F. Marenkin [2], Sh.B. Abdulvagidov [1], U.Z. Zalibekov [1]

[1] Amirkhanov Institute of Physics, Daghestan Federal Research Center, Russian Academy of Sciences, Makhachkala, Russia
[2] Kurnakov Institute of General and Inorganic Chemistry, Russian Academy of Sciences, Moscow, Russia

E-mail: uzvideo@inbox.ru

Received March 20, 2024
Revised March 26, 2024
Accepted March 27, 2024

The paper presents the results of an experimental study of the electrical resistivity $\rho(P)$, the Hall coefficient $R_H(P)$ and the transverse magnetoresistance $\Delta\rho_{xx}/\rho_0(P)$ of the heterogeneous alloy $Cd_3As_2(MnAs)_{0.03}$ at hydrostatic pressure up to 9 GPa at room temperature. Features of the behavior of $\rho(P)$, $R_H(P)$ and $\Delta\rho_{xx}/\rho_0(P)$ $Cd_3As_2(MnAs)_{0.03}$, which are associated with phase transitions in Cd_3As_2 and MnAs, were observed in the pressure range $P \approx (1.6-2.7)$ GPa. Maxima of negative and positive magnetoresistance (MR) discovered during measurements of MR with increasing and decreasing pressure. With increasing magnetic field, a significant increase in negative MR is observed. In the pressure region of 1.6−2.8 GPa, the maximum negative MC ≈ 10% was observed at $P \approx 2.2$ GPa.

Keywords: high pressure, resistivity, Hall coefficient, magnetoresistance, phase transition.

DOI: 10.61011/PSS.2024.05.58496.62

1. Introduction

Sufficient attention is currently paid to the investigation of negative magnetoresistance (NMR) in magnetic and non-magnetic materials. Various models are proposed for description of this phenomenon that consider or not consider the presence of impurities in materials. In studies investigating NMR in graphene, high NMR mechanism together with traditional models are associated with disordering, rather than with magnetism [1,2].

In narrow-bandgap semiconductors, dependence of degree of order or disorder of mobile electrons on magnetic field is defined by the type of MS [3]: magnetic fiels orders almost free electrons, i. e. arranges their spins in „ferromagnetic" order resulting in the appearance of negative MS. Negative MS in the topological insulator $TlBi_{0.15}Sb_{0.85}Te_2$ is induced by the Zeeman effect [3] resulting in the appearance of cluster-like variation of the electronic structure. In this clusters, electron spins are codirectional, therefore, resistance in them becomes a little lower and negative MS occurs.

Some authors correlate the occurrence of NMR with the fact that electrons will be less scattered in polycrystals or materials with many defects in the form of, for example, plate-type surfaces, etc., in case when the electron path curvature radius is lower as the magnetic field induction increases, and, therefore, probability of collision with the scattering planes will be lower and path length will grow [4].

Many researchers correlate the occurrence of NMR with the presence of phase transitions, which is close to our opinion [5–7]. This study investigates heterogeneous $Cd_3As_2(MnAs)_{0.03}$ alloy as a promising research area. Cd_3As_2 was for the first time addressed as a narrow-bandgap semiconductor with abnormally high mobility of electrons. Quite recently, Cd_3As_2 was rediscovered as 3*D* topological semimetal positioned as a bulk equivalent of graphene that has NMR and superconductivity. Conduction band and valence band of Cd_3As_2 have a linear dispersion law and contact each other in the 3D Brillouin zone forming the Dirac points. On the assumption of time inversion and inverted symmetry, the Dirac points are doubly degenerate. Asymmetry results in splitting the Dirac point. The magnetic field transforms the Weyl semimetal by generating NMR and inducing superconducting properties.

We have investigated the effect of hydrostatic pressure on kinetic properties of $Cd_3As_2(MnAs)_{0.03}$. The paper describes the experimental study of specific electrical resistance $\rho(P)$, Hall coefficient $R_H(P)$ and transverse magnetoresistance $\Delta\rho_{xx}/\rho_0(P)$ of $Cd_3As_2(MnAs)_{0.03}$ at hydrostatic pressure up to 9 GPa of the pressure in the room temperature range.

2. Experimental procedure and technique

$Cd_3As_2(MnAs)_{0.03}$ bulk crystals were synthesized by the vacuum vial method from Cd_3As_2 and MnAs at MnAs melting temperature [8]. Structure and composition of samples, and distribution of elements on the surface were examined using JSM-6610LV (Jeol) scanning election microscope (SEM) with X-MaxN (Oxford Instruments) energy-dispersive X-ray spectroscopy (EDXRS) module.

Secondary and back-scattered electron detectors were used for measurement. Measurements at high pressure up to 9 GPa were made using Toroid unit [9] at room temperatures.

3. Measurements and discussion

XPA diffraction pattern of $Cd_3As_2(MnAs)_{0.03}$ shown in Figure 1 well identifies two phases: α-Cd_3As_2 ($I4_1cd$, sp. gr. 110) with tetragonal structure and MnAs with hexagonal structure ($P6_3/mmc$, sp. gr. 194).

Figure 2 shows pressure dependences of specific electrical resistance $\rho(P)$ measured at room temperature (300 K) in $Cd_3As_2(MnAs)_{0.03}$ in compression and decompression conditions. At $P \geq 1.5$ GPa $\rho(P)$ varies a little and achieves its peak at $P \approx 1.95$ GPa associated with phase transition. With further growth of pressure up to 8 GPa, $\rho(P)$ grows much faster and, when pressure drops, a minimum value is observed at $P \approx 2.7$ GPa. Changes of $\rho(P)$ are reversible, i. e., when pressure is released, resistance returns almost to its initial values. Nonexistent or almost nonexistent hysteresis indicates that the phase transition in the neighbourhood of 1.75–2.7 GPa is either an electronic transition or weak 1-order structural transition close to 2-order transition where crystal symmetry varies, while relative change of lattice cell volumes before and after transition is negligible or absent. It should be noted that the transition width in compression (0.7 GPa) is much wider then in decompression (0.1 GPa), showing that pressure results in ordering or defect annihilation in the sample (blue curve is below the red curve).

The available information on electrotransport in Cd_3As_2 at high pressures [10–12] indicates pronounced changes in the pressure range 2.5–4 GPa. The tetragonal phase occurs at ≈ 2.5 GPa, while the monoclinic phase is localized at ≈ 4 GPa [10]; semimetal–semiconductor phase transition takes place at 2.5 GPa. In another study [11], Cd_3As_2 demonstrates the semimetal–semiconductor behavior at much lower pressure (1.1 GPa) compared with the observed structural phase transition within 2.6–4.67 GPa. In addition, for pressures higher than 8.5 GPa, a low-temperature superconducting phase is observed, thus, supporting a previous proposal of Cd_3As_2 as a candidate for topological superconductivity. So, electrical transport measurements in Cd_3As_2 show contradictory interpretations of high pressure phase.

$Cd_3As_2(MnAs)_{0.03}$ investigated herein — is a new little known and underinvestigated semimagnetic semiconductor. Pressure analysis of specific electrical resistance of $Cd_3As_2(MnAs)_{0.03}$ indicates a semimetal nature of conductance. Hydrostatic pressure shall result in decrease of semimetal overlapping of energy bands. Actually, our measurements show that under pressure overlapping decreases and resistance increases. To get additional information on the type of change of transport properties of $Cd_3As_2(MnAs)_{0.03}$ with pressure, we have also measured the hall effect and magnetoresistance in the perpendicular magnetic field.

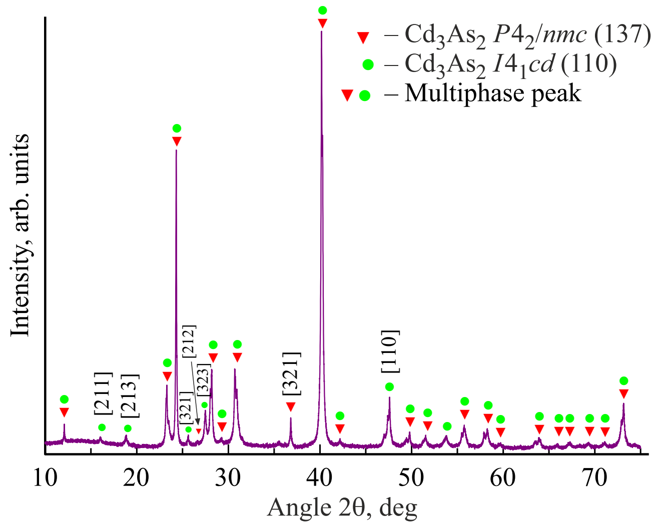

Figure 1. Diffraction pattern of the sample $Cd_3As_2(MnAs)_{0.03}$.

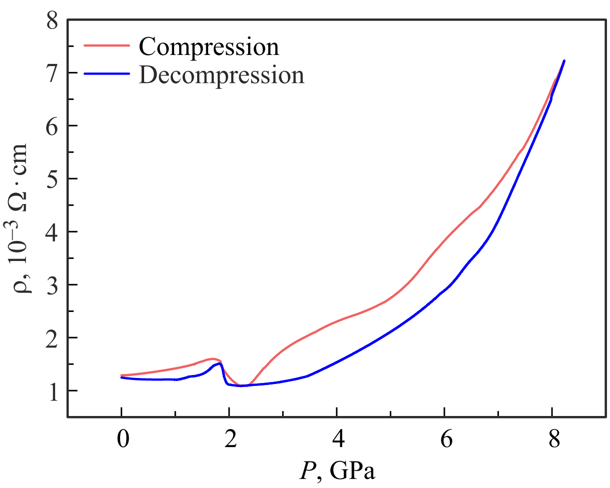

Figure 2. Specific electrical resistance curves of $Cd_3As_2(MnAs)_{0.03}$ in compression and decompression.

Figure 3 shows pressure dependences of the Hall coefficient $R_H(P)$ measured in magnetic fields (1000–5000) Oe at room temperature. $R_H(P)$ satisfactorily correlates with $\rho(P)$. In $Cd_3As_2(MnAs)_{0.03}$, the Hall coefficient up to $P \approx 2.2$ GPa reaches its peak and then drops and has its valley at $P \approx 5.3$ GPa.

Figure 4 shows the variation of magnetotransport in $Cd_3As_2(MnAs)_{0.03}$ with pressure. With growth of magnetic field, considerable increase of negative magnetoresistance is observed. Maximum NMR $\approx 10\%$ at ≈ 2.2 GPa was observed within 1.6–2.8 GPa. Such magnetoresistance behavior that agrees with the observed feature of electrical resistance behavior near 1.75–2.7 GPa (Figure 2) is induced by the structural phase transition detected by us.

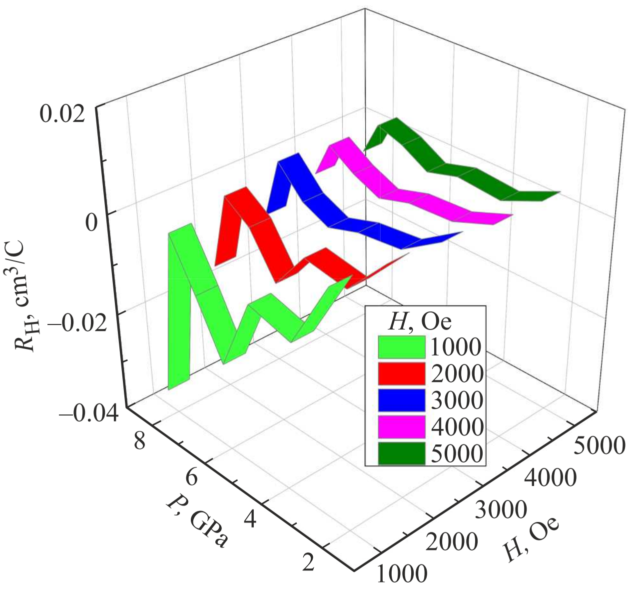

Figure 3. Pressure dependences of the Hall coefficient R_{H0}.

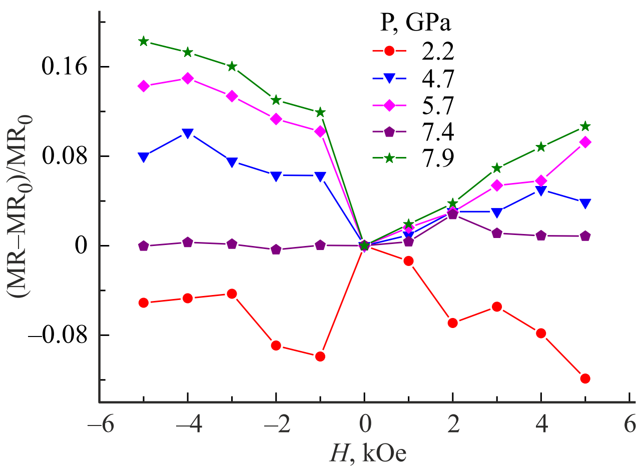

Figure 4. Pressure-MS dependences at various magnetic field strengths.

Correlation of the effect of pressure and magnetic field on the NMR coefficient in $Cd_3As_2(MnAs)_{0.03}$ is obvious. However, the figure shows that the effect of the magnetic field on electrical resistance is much less pronounced. Nevertheless, phase transition is also observed in plane (H vs. MR), but only near 2000 Oe. Thus, the phase transition, that exists without magnetic field at 2 GPa, is enhanced as the magnetic field grows up to 5000 Oe, while in field 2000 Oe (red curve) abnormal decrease of MR is observed. Compared with the pressure, the degree of changes in magnetic field is by an order of magnitude lower. This is because the internal negative pressure (chemical pressure in the magnetic field) induced by magnetoactive cations oriented by the magnetic field is also much lower. However, Cd_3As_2 matrix in $Cd_3As_2(MnAs)_{0.03}$ is paramagnetic and, therefore, the chemical pressure induced by the magnetic field has no any significant effect on the band structure of the Dirac semiconductor Cd_3As_2, no less an effect that is capable of inducing the observed phase transitions. hydrostatic pressure considerably reduces interatomic distances and, thus, as is commonly known, has a considerable effect on the band gap, but changes the arrangement of the valence band top and valence band bottom in the wave k-space. Moreover, the effects of transformation of the Dirac semimetal into the Weyl semimetal by the magnetic field resulting in the generation of NMR and superconductivity take place near the absolute zero temperature and in very strong magnetic fields, which is not observed in conditions of our experiment with a heterogeneous alloy. $Cd_3As_2(MnAs)_{0.03}$.

Thus, it remains to discuss the mechanism of spin polarization by ferromagnetic MnAs nanoclusters through Cd_3As_2matrix of globular$Cd_3As_2(MnAs)_{0.03}$ alloy as proposed by us in [13]. Current flowing through the paramagnetic medium containing ferromagnetic inclusions becomes spin-polarized. ferromagnetic Co spin-polarizes the current in heterogeneous Cu-Co alloy [14], in ferromagnetic- superconductor heterojunction $La_{0.7}Sr_{0.3}MnO_3/SrTiO_3/Nb$ [15], in point contact of ferromagnetic and superconductor [16]. Performance of spintronic devices depends on the degree of spin polarization of carriers injected from ferromagnetic and on the length on which the current is still spin-polarized in the paramagnetic medium. Magnetoelectronic devices will have their best performance when the initial (near the ferromagnetic surface) spin polarization is maximum and when the spin polarization of current decreasing with distance nevertheless remains quite high to achieve topologically significant magnetization of the adjacent ferromagnetic that depends on the free path length and electron mobility in the paramagnetic medium. Semimetal ferromagnetic materials based on 3*d* metals induce approx 2 times higher and almost 100% polarization of spin current than the same elements in pure form [16]. it is reasonable to expect that the spin polarization in MnAs is $\approx 100\%$. Moreover, Cd_3As_2 matrix itself, having a large free path length of current carriers (see below) and high mobility [17], $2 \cdot 10^4\,cm^2/V \cdot s$, almost does not reduce the spin polarization of intercluster current. Thus, the processing properties of $Cd_3As_2(MnAs)_{0.03}$ are the best for spintronics devices, including terahertz devices [18–20], and $T_C = 318\,K$ in MnAs allows them to function in ambient conditions.

We have found that in $Cd_3As_2(MnAs)_{0.03}$ with typical diameter of MnAs cluster 5 nm the distance between them is approx 50 nm. These data are approximately the same as those in the heterogeneous Cu-Co alloy [14] with 5-nm cobalt clusters inside the copper matrix. In Cu-Co alloy NMR at 100 K is max. 7%, while for the previously investigated $Cd_3As_2(MnAs)_{0.447}$ NMR achieves 2% in 4.5 T magnetic field at room temperature, which is probably due to the fact that Cd_3As_2 matrix, owing to the unparalleled properties as mentioned above, retains the induced spin polarization much better than Cu.

4. Conclusion

Experimental investigations of specific electrical resistance $\rho(P)$, Hall coefficient $R_H(P)$ and transverse magnetoresistance $\Delta\rho_{xx}/\rho_0(P)$ were performed in heterogeneous $Cd_3As_2(MnAs)_{0.03}$ alloy where at high hydrostatic pressures up to 9 GPa and in the room temperature region stepwise changes inherent in phase transitions were detected suggesting that a pressure-induced phase transition takes place in the test sample. Pressure dependences of transverse magnetoresistance $\Delta\rho_{xx}/\rho_0(P)$ were studied. They quite possibly exhibit spin polarization of intrinsic carriers of Cd_3As_2 matrix, induced by Mn cations as well as MnAs clusters, whose presence is confirmed by, though small, peak on XPA. The effect of the magnetic field on electrical resistance is much less pronounced compared with the pressure. At $P = 2$ GPa, the maximum increase of NMR in absolute value is observed in 5000 Oe field. To study this phenomenon, further detailed investigations of magnetic and structural properties in the pressure range of 1.75–2.7 GPa are required.

Conflict of interest

The authors declare that they have no conflict of interest.

References

[1] M. Gibertini, A. Tomadin, F. Guinea, M.I. Katsnelson, M. Polini. Phys. Rev. B **85**, 201405(R) (2012).
[2] J. Martin, N. Akerman, G. Ulbricht, T. Lohmann, J.H. Smet, K. von Klitzing, A. Yacoby. Nature. Phys. **4**, 144 (2008).
[3] O. Breunig, Z. Wang, A.A. Taskin, J. Lux, A. Rosch, Y. Ando. Nature Commun. **8**, 15545 (2017) DOI: 10.1038/ncomms15545.
[4] Y. Zhou, B. Han, Z. Liao, H. Wu, D. Yu. App. Phys. Lett. **98**, 222502 (2011).
[5] Sh.M. Alekperova, I.A. Akhmedova, G.S. Gadzhieva, Kh.D. Dzhalilova. FTT **49**, *3*, 490 (2007). (in Russian).
[6] I.G. Gorlova, V.Ya. Pokrovsky, S.Yu. Gavrilkin, A.Yu. Tsvetkov. Pisma v ZhETF **107**, *3*, 180 (2018). (in Russian).
[7] R.K. Arslanov, T.R. Arslanov, I.V. Fedorchenko, L. Kilansky, T. Chatterdzhi. ZhETF **107**, *10*, 643 (2018). (in Russian).
[8] A.I. Rul', A.V. Kochura, S.F. Marenkin. Izv. Yugo-Zapadnogo gos. un-ta. Ser. Tekhnika i tekhnologii, **7**, 120 (2017). (in Russian).
[9] L.G. Khvostantsev, V.N. Slesarev, V.V. Brazhkin. High Pressure Res. **24**, 371 (2004).
[10] S. Zhang, Q. Wu, L. Schoop, M.N. Ali, Y. Shi, N. Ni, Q. Gibson, S. Jiang, V. Sidorov, W. Yi, J. Guo, Y. Zhou, D. Wu, P. Gao, D. Gu, C. Zhang, S. Jiang, K. Yang, A. Li, Y. Li, X. Li, J. Liu, X. Dai, Z. Fang, R.J. Cava, L. Sun, Z. Zhao. Phys. Rev. **91**, 165133, (2015).
[11] L. He, Y. Jia, S. Zhang, X. Hong, C. Jin, S. Li. Quantum Mater. **1**, 16014 (2016).
[12] C. Zhang, J. Sun, F. Liu, A. Narayan, N. Li, X. Yuan, Y. Liu, J. Dai, Y. Long, Y. Uwatoko, J. Shen, S. Sanvito, W. Yang, J. Cheng, F. Xiu. Phys. Rev. B **96**, 155205, (2017).
[13] Sh.B. Abdulvagidov, L.A. Saypulaeva, A.I. Ril. Solid State Commun. (under consideration).
[14] A.E. Berkowitz, J.R. Mitchell, M.J. Carey, A.P. Young, S. Zhang, F.E. Spada, F.T. Parker, A. Hutten, G. Thomas. Phys. Rev. Lett. **68**, c. 3745 (1992).
[15] L. Fratila, I. Maurin, C. Dubourdieu, J.C. Villégier. Appl. Phys. Lett. **86**, 122505-3 (2005).
[16] R.J. Soulen Jr., J.M. Byers, M.S. Osofsky, B. Nadgorny, T. Ambrose, S.F. Cheng, P.R. Broussard, C.T. Tanaka, J. Nowak, J.S. Moodera, A. Barry, J.M.D. Coey. Science **282**, 85 (1998).
[17] J. Cao, S. Liang, C. Zhang, Y. Liu, J. Huang, Z. Jin, Z. Chen, Z. Wang, Q. Wang, J. Zhao, Sh. Li, X. Dai, J. Zou, Zh. Xia, L. Li, F. Xiu. Nature Commun. **6**, 7779 (2015).
[18] C. Spezzani, E. Ferrari, E. Allaria, F. Vidal, A. Ciavardini, R. Delaunay, F. Capotondi, E. Pedersoli, M. Coreno, C. Svetina, L. Raimondi, M. Zangrando, R. Ivanov, I. Nikolov, A. Demidovich, M.B. Danailov, H. Popescu, M. Eddrief, G. De Ninno, M. Kiskinova, M. Sacchi. Phys. Rev. Lett. **113**, 247202 (2014).
[19] J. Hubmann, B. Bauer, H.S. Korner, S. Furthmeier, M. Buchner, G. Bayreuther. Nano Lett. **16**, 900 (2016).
[20] V.M. Novotortsev, S.F. Marenkin, I.V. Fedorchenko, A.V. Kochura. Russ. J. Inorg. Chem. **55**, C. 1762 (2010).

Translated by E.Ilinskaya